

V.F. Bolyukh, O.I. Kocherga

## Efficiency of multi-armature linear pulse electromechanical power and speed converters

**Introduction.** High-speed linear pulse electromechanical converters (LPEC) provide acceleration of the executive element in a short active section to high speed with significant displacement, while power-purpose LPECs create powerful power impulses of the executive element on the object of influence with minor movements. One of the areas of improvement of LPEC is the creation of multi-armature structures. **Methodology.** To analyze the electromechanical characteristics and indicators of LPEC, a mathematical model was used, which takes into account the interconnected electrical, magnetic, mechanical and thermal processes that occur when connected to a pulse energy source with a capacitive energy storage. The main results of the calculations were performed in the COMSOL Multiphysics software environment and confirmed by experimental studies in laboratory conditions. **Results.** The features of the electromechanical processes of multi-armature LPECs are established and their indicators are determined. With the help of efficiency criteria, which take into account electrical, power, speed and magnetic indicators in a relative form with different options for their evaluation strategy, it was established that multi-armature LPECs for power purposes have increased efficiency, and for high-speed LPECs the use of multi-armature configurations is impractical. The conducted experimental studies confirm the reliability of the calculated results. **Originality.** It has been established that almost all multi-armature LPECs for power purposes have higher efficiency compared to a converter with one armature, and for high-speed LPECs it is advisable to use traditional LPECs with one armature. **Practical value.** On the basis of multi-armature LPECs, models of an electromagnetic UAV catapult, a magnetic pulse press for ceramic powder materials, an electromechanical device for dumping ice and snow deposits from a power line wire, a device for destroying information on a solid-state digital SSD drive have been developed and tested. References 20, tables 4, figures 8.

**Key words:** linear pulsed electromechanical converter, multi-armature configuration, continuous electrically conductive armature, coil armature, ferromagnetic armature, efficiency criterion, experimental studies.

**Вступ.** Лінійні імпульсні електромеханічні перетворювачі (ЛІЕП) швидкісного призначення забезпечують розгін виконавчого елемента на короткій активній ділянці до високої швидкості зі значним його переміщенням, а ЛІЕП силового призначення створюють потужні силові імпульси виконавчим елементом на об'єкт впливу при незначних його переміщеннях. Одним із напрямків удосконалення ЛІЕП є створення багатоякірних конструкцій. **Методика.** Для аналізу електромеханічних характеристик та показників ЛІЕП використана математична модель, в якій враховані взаємопов'язані електричні, магнітні, механічні та теплові процеси, які виникають при підключенні до імпульсного джерела енергії з ємнісним накопичувачем енергії. Основні результати розрахунків виконані в програмному середовищі COMSOL Multiphysics і підтверджені експериментальними дослідженнями в лабораторних умовах. **Результати.** Встановлені особливості електромеханічних процесів багатоякірних ЛІЕП та визначено їх показники. За допомогою критеріїв ефективності, які у відносному вигляді враховують електричні, силові, швидкісні та магнітні показники при різних варіантах стратегії їх оцінки, встановлено, що багатоякірні ЛІЕП силового призначення мають підвищену ефективність, а для ЛІЕП швидкісного призначення використання багатоякірних конфігурацій недоцільно. Проведені експериментальні дослідження підтверджують достовірність розрахункових результатів. **Наукова новизна.** Встановлено, що практично всі багатоякірні ЛІЕП силового призначення мають більшу високу ефективність в порівнянні з перетворювачем з одним якорем, а для ЛІЕП швидкісного призначення доцільно застосовувати традиційні ЛІЕП з одним якорем. **Практична цінність.** На базі багатоякірних ЛІЕП розроблено та випробувано моделі електромагнітної катапульти БПЛА, магітно-імпульсного пресу для керамічних порошкових матеріалів, електромеханічного пристрою для скидання ожеледних і снігових відкладень з проводу лінії електропередачі, пристрою для знищення інформації на твердотільному цифровому SSD накопичувачі. Бібл. 20, табл. 4, рис. 8.

**Ключові слова:** лінійний імпульсний електромеханічний перетворювач, багатоякірна конфігурація, суцільний електропровідний якір, котушковий якір, феромагнітний якір, критерій ефективності, експериментальні дослідження.

**Introduction.** One of the promising devices of modern electromechanics are linear pulse electromechanical converters (LPEC) for speed and power purposes. High-speed LPECs provide acceleration of the executive element in a short active section to high speed with significant movement of it, and power LPECs create powerful power impulses of the executive element on the object of influence with minor movements [1-4].

LPECs are characterized by significant electromagnetic and mechanical loads, which significantly exceed similar indicators of traditional linear electric motors with long-term operation. They are used in many areas of science, technology and security. Among the technological applications, it is possible to mention shock-condenser welding, metal processing, stamping, riveting, assembly and forming operations, etc. These converters are used for testing systems for shock loads, high-speed electrical devices, destruction of information in case of unauthorized access, valve and switching equipment, seismic sources, cleaning of bunkers from remaining materials and power lines from icing, launchers, etc. [5-10].

In the coaxial LPEC, opposite the disk inductor winding (IW), which is excited by current from a pulsed electric source with a capacitive energy storage (CES), a disk armature is located, which moves in the axial direction. The most widespread are induction, electromagnetic and electrodynamic types of LPEC.

In the induction-type LPEC, the armature is made solid in the form of a thin conductive disk. In the LPEC of the electrodynamic type, the armature is made in the form of a multi-turn coil, which is connected in series or in parallel with the IW. In the LPEC of the electromagnetic type, the armature is made in the form of a relatively thick ferromagnetic disk.

In the LPEC of the electromagnetic type, electromagnetic forces (EMF) of attraction act on the ferromagnetic armature (FA) from the side IW. In the LPEC of the electrodynamic type, electrodynamic forces (EDF) of repulsion arise between the coil armature (CA) and the stationary IW. In the induction-type LPEC, when the magnetic field IW interacts with the induced current

© V.F. Bolyukh, O.I. Kocherga

in the solid electrically conductive armature (EA), a repulsive EDF occurs.

The specified LPECs are characterized by different speeds of electromagnetic processes, different directions of action of electrodynamic and electromagnetic forces relative to IW, etc. In order to strengthen the power effect and increase the speed indicators, ferromagnetic cores and shields, additional secondary windings, mechanical power elements, cryogenic cooling, etc. are used in LPEC [11-13]. But the analysis of the specified types of LPEC with a traditional configuration with one armature showed that their efficiency remains at a rather low level and their efficiency when working as an accelerator does not exceed 10-15 % [14].

One of the areas of improvement of LPEC is the creation of multi-armature structures [15, 16]. In [17], a LPEC with two EA, which form an increased pulse of mechanical force on two opposite sides, is described. The work [18] presents the design scheme of LPEC, which consists of two stationary IW and movable EA and FA. The armatures are interconnected through a system of rods, which in turn are connected to the executive element. But the lack of a comprehensive study of the electromechanical characteristics and main indicators of multi-armature LPECs makes it impossible to determine effective configurations for various purposes.

The **purpose** of the work is to determine configurations of LPEC that provide increased efficiency due to the use of several armatures interacting with an inductor that is excited by a pulsed source of energy from CES.

Multi-armature LPECs must provide a unidirectional force on the executive element at high-speed assignment or the summation of all forces at the power assignment of the converter.

**Mathematical model of LPEC.** Interrelated electromagnetic, thermal and mechanical processes occur in LPEC, which occur when connected to a pulse energy source from CES.

We consider that the coaxial LPEC has a disk IW and the movement of the disk armatures is carried out along the  $z$  axis. Consider the LPEC, which includes stationary IW and FA, moving CA and EA. For the instantaneous values of the tangential component of the vector magnetic potential  $A_\varphi$  in the cylindrical coordinate system, we write down the system of differential equations:

$$\gamma_1 \frac{\partial A_{1\varphi}}{\partial t} + \frac{\partial}{\partial z} \left( \frac{1}{\mu_0} \frac{\partial A_{1\varphi}}{\partial z} \right) + \frac{\partial}{\partial r} \left( \frac{1}{\mu_0 r} \frac{\partial (r A_{1\varphi})}{\partial r} \right) = -j_1(t); \quad (1)$$

$$\gamma_2 \frac{\partial A_{2\varphi}}{\partial t} + \frac{\partial}{\partial z} \left( \frac{1}{\mu_0} \frac{\partial A_{2\varphi}}{\partial z} \right) + \frac{\partial}{\partial r} \left( \frac{1}{\mu_0 r} \frac{\partial (r A_{2\varphi})}{\partial r} \right) - \quad (2)$$

$$-v_2(t) \frac{\gamma_2}{\mu_0} \frac{\partial A_{2\varphi}}{\partial z} = -j_2(t);$$

$$\gamma_3 \frac{\partial A_{3\varphi}}{\partial t} + \frac{\partial}{\partial z} \left( \frac{1}{\mu_0} \frac{\partial A_{3\varphi}}{\partial z} \right) + \frac{\partial}{\partial r} \left( \frac{1}{\mu_0 r} \frac{\partial (r A_{3\varphi})}{\partial r} \right) - \quad (3)$$

$$-v_3(t) \frac{\gamma_3}{\mu_0} \frac{\partial A_{3\varphi}}{\partial z} = 0;$$

$$\gamma_4 \frac{\partial A_{4\varphi}}{\partial t} + \frac{\partial}{\partial z} \left( \frac{1}{\mu_4} \frac{\partial A_{4\varphi}}{\partial z} \right) + \frac{\partial}{\partial r} \left( \frac{1}{\mu_4 r} \frac{\partial (r A_{4\varphi})}{\partial r} \right) = 0, \quad (4)$$

$$\frac{\partial}{\partial z} \left( \frac{1}{\mu_0} \frac{\partial A_{5\varphi}}{\partial z} \right) + \frac{\partial}{\partial r} \left( \frac{1}{\mu_0 r} \frac{\partial (r A_{5\varphi})}{\partial r} \right) = 0, \quad (5)$$

where the index of the element (space)  $n = 1 - IW, 2 - CA, 3 - FA, 4 - FA, 5 - \text{airspace}$ ;  $i_1(t), i_2(t)$  - currents IW and CA, respectively;  $j_1(t) = i_1(t)N_1S_1^{-1}k_1, j_2(t) = i_2(t)N_2S_2^{-1}k_2$  - current density IW and CA, respectively;  $\gamma_n$  - specific conductivity of the material of the  $n^{\text{th}}$  element;  $\mu_0$  - magnetic constant;  $\mu_4$  - magnetic permeability FA;  $v_2(t), v_3(t)$  - speed CA and EA, respectively;  $N_1, N_2$  - the number of turns IW and CA, respectively;  $S_1, S_2$  - cross-sectional area IW and CA, respectively;  $k_1, k_2$  - filling factor IW and CA, respectively.

Differential equations (1) - (5) are supplemented with boundary and initial conditions.

To calculate the axial component of the force acting on the corresponding LPEC armature, we use Maxwell's tension tensor:

$$f_z = \oint_S 2\pi r T_z ds = \frac{1}{\mu_0} \oint_S 2\pi r (B_r \cdot B_z) ds, \quad (6)$$

where  $B_r = -\frac{\partial A_\varphi}{\partial z}, B_z = \frac{1}{r} \frac{\partial (r A_\varphi)}{\partial r}$  are components of the magnetic field induction vector  $\mathbf{B}$ .

The electrical circuit of the LPEC with the serial connection of the stationary IW with the movable CA, which interacts with the movable EA, can be represented by the substitution diagram (Fig. 1) and described by the system of equations:

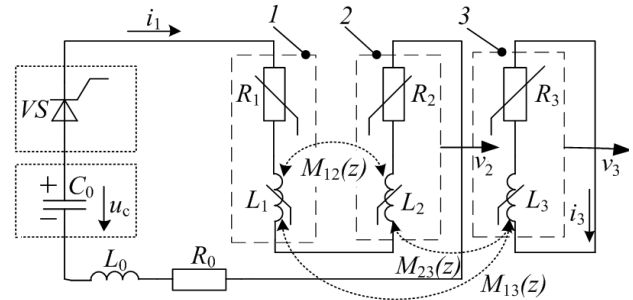


Fig. 1. Electrical diagram of LPEC with a series connection of IW (1) with CA (2), which interacts with EA (3)

$$2\pi \frac{N_1}{S_1} \cdot \int_{S_1} \frac{dr A_{1\varphi}}{dt} dr dz + 2\pi \frac{N_2}{S_2} \cdot \int_{S_2} \frac{dr A_{2\varphi}}{dt} dr dz + L_0 \frac{di_1}{dt} + \quad (7)$$

$$+ i_1 [R_0 + R_1(T_1) + R_2(T_2)] + u_c = 0;$$

$$2\pi \frac{N_3}{S_3} \cdot \int_{S_3} \frac{dr A_{3\varphi}}{dt} dr dz + i_3 R_3(T_3) = 0; \quad (8)$$

$$\frac{du_c}{dt} = \frac{i_1}{C_0}, \quad (9)$$

where  $R_0, L_0$  - resistance and inductance of power cables, respectively;  $R_1(T_1), R_2(T_2), R_3(T_3)$  - resistance IW, CA and EA, respectively;  $T_1, T_2, T_3$  - temperature IW, CA and EA, respectively;  $i_3$  - current EA;  $u_c$  - voltage of CES;  $C_0$  - CES capacity;  $S_3$  - cross-sectional area EA.

The system of equations describing the electrical and magnetic connections between the active elements of the LPEC in parallel connection of IW with movable CA, which interacts with movable EA, takes the following form:

$$2\pi \frac{N_1}{S_1} \cdot \int_{S_1} \frac{dr A_{1\varphi}}{dt} dr dz + L_0 \frac{di}{dt} + R_0 i + i_1 R_1(T_1) + u_C = 0; \quad (10)$$

$$2\pi \frac{N_2}{S_2} \cdot \int_{S_2} \frac{dr A_{2\varphi}}{dt} dr dz + L_0 \frac{di}{dt} + R_0 i + i_2 R_2(T_2) + u_C = 0; \quad (11)$$

$$2\pi \frac{N_3}{S_3} \cdot \int_{S_3} \frac{dr A_{3\varphi}}{dt} dr dz + i_3 R_3(T_3) = 0; \quad (12)$$

$$\frac{du_c}{dt} = \frac{i}{C_0}, \quad (13)$$

where  $i(t) = i_1(t) + i_2(t)$  – current of CES.

The mechanical processes of LPEC are described by a system of equations:

$$(m_3 + m_e) \frac{dv_3}{dt} = f_3(t) - K_{mp} v_3(t); \quad (14)$$

$$(m_3 + m_2 + m_e) \frac{dv_2}{dt} = f_2(t) - K_{mp} [v_3(t) + v_2(t)] - K_B [v_3(t) + v_2(t)]^2 - K_P [z_3(t) + z_2(t)], \quad (15)$$

where  $m_2, m_3, m_e$  – the mass of CA, EA and the executive element, respectively;  $z_2(t), z_3(t)$  – moving CA and EA, respectively;  $f_2(t), f_3(t)$  – EDF on CA and EA, respectively;  $K_{mp}$  – coefficient of dynamic friction;  $K_B$  – drag coefficient;  $K_P$  – coefficient of elasticity of the return element (spring).

The system of equations (14), (15) is supplemented by the corresponding initial conditions.

The temperature  $T_n$  in the  $n^{\text{th}}$  active current-conducting element of the LPEC is described as:

$$c_n(T) \gamma_n \frac{\partial T_n}{\partial t} = \lambda_n(T) \left( \frac{\partial^2 T_n}{\partial r^2} + \frac{1}{r} \frac{\partial T_n}{\partial r} + \frac{\partial^2 T_n}{\partial z^2} \right) + j_n^2(t) k_n \rho_n(T), \quad (16)$$

where  $c_n(T), \gamma_n, \lambda_n(T), \rho_n(T)$  – specific heat capacity, material density, thermal conductivity coefficient, specific resistance of the  $n^{\text{th}}$  active element.

On the cooled surfaces of the active elements, the system of equations (16) is supplemented by boundary conditions of the third kind, and on the axis of symmetry of the LPEC by boundary conditions of the second kind. To implement the mathematical model, a system of partial differential equations with respect to spatial and temporal variables is used using the software package Comsol Multiphysics 5.3.

#### Analysis of indicators of multi-armature LPEC.

For the analysis of LPEC, we introduce the following notations. In the presence of a continuous conductive armature, «E» is added, in the presence of a coil armature, «C», and in the presence of a ferromagnetic armature, «F». We will analyze multi-armature converters with two armatures (LPEC-E2, LPEC-C-E, LPEC-E-F, LPEC-C-F) and three armatures (LPEC-C-E2, LPEC-C-E-F). With a parallel connection, CA with IW –  $C_p$ , with a serial connection –  $C_s$ . CA and IW are wound in opposite directions so that repulsion forces act between them.

Let's consider the electromechanical characteristics of LPEC with the following parameters. IW (CA): outer

diameter  $D_{ex1}=100$  mm, inner diameter  $D_{in1}=10$  mm, height  $H_1=10$  mm, number of turns  $N_1=46$ , cross section of copper bus  $S_1=a_1 \cdot b_1=1.8 \cdot 4.8=8.64$  mm<sup>2</sup>. EA: material – copper M2, outer diameter  $D_{ex3}=100$  mm, inner diameter  $D_{in3}=10$  mm, height  $H_3=3$  mm. FA: material – Steel 3, outer diameter  $D_{ex4}=100$  mm, inner diameter  $D_{in4}=10$  mm, height  $H_4=12$  mm. The distance between IW and CA  $h_{12}=2$  mm, between CA and EA  $h_{23}=2$  mm. The power source includes a CES with parameters  $C_0=2500$  μF,  $U_0=450$  V and a reverse diode that provides a polar aperiodic pulse of the excitation current [19].

We will use the following designations of elements. Active elements: 1 – IW, 2 – front EA, 3 – rear EA, 4 – CA, 5 – FA. Passive elements: 6 – executive element, 7 – movable or immovable fixators, 8 – object of influence, 9 – internal power ferromagnetic device (Fig. 2).

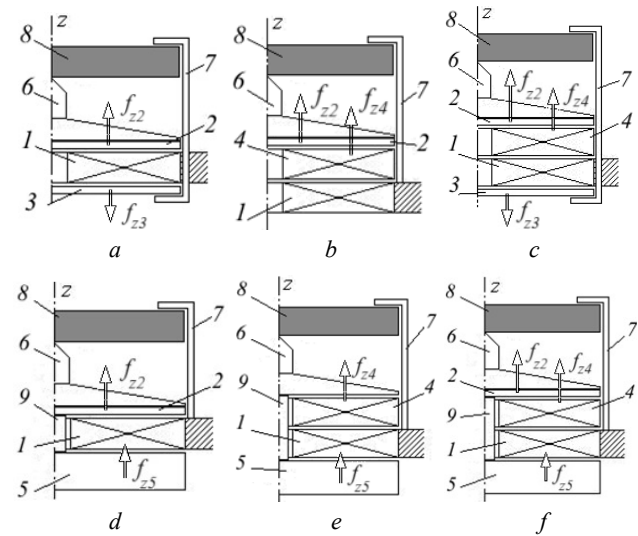


Fig. 2. Design schemes of multi-armature LPEC for power purposes: LPEC-E2 (a), LPEC-C-E (b), LPEC-C-E2 (c), LPEC-E-F (d), LPEC-C-F (e), LPEC-C-E-F (f)

In multi-armature LPECs of power purpose, slow-moving armatures transmit axially directed force to the object of influence through an executive element in the form of a striker, external fasteners and internal power devices.

For the LPEC of power purpose, we will conduct an analysis of the amplitude  $f_{zm}$  and the magnitude of the impulse  $F_z = \int f_z(z,t) dt$  of axial electrodynamic and electromagnetic forces that are transmitted to the object of influence.

In LPEC-E2, two EA cover IW from opposite sides and act on the movable latch, forming oppositely directed EDF repulsions of the front  $2 f_{z2}$  and rear  $3 f_{z3}$  EA (Fig. 2,a). In this LPEC, the current density in IW  $j_1$  has the form of a polar aperiodic pulse, while the current density in the front  $j_2$  and in the back  $j_3$  EA for 1.3 ms have the opposite polarity. The amplitude of the current density in IW  $j_{1m}=266.7$  A/mm<sup>2</sup>, and in the armatures  $-j_{2,3m}=390.2$  A/mm<sup>2</sup>. The EDF pulses acting on the front  $F_{z2}$  and rear  $F_{z3}$  EA have the opposite polarity. The EDF amplitudes acting between the two EA are  $f_{z2,3m}=8.55$  kN, and the magnitude of the EDF pulse is  $F_{z2,3}=3.3$  N·s. The total force is transmitted from armatures 2 and 3 to the impact object 8 with the help of movable retainers 7.

In the LPEC-C<sub>p</sub>-E with the front EA and CA, which is connected in parallel with IW, the force is transmitted to the fixed retainer (Fig. 2,b). With such a connection, the magnitudes of the currents in IW and CA differ due to induction interaction with EA. EDF acting on EA  $f_{z2}$  and CA  $f_{z4}$  form corresponding EDF pulses  $F_{z2}$  and  $F_{z4}$ . Amplitudes of EDF acting on EA  $f_{z2m}=7.28$  kN, and on CA  $f_{z4m}=5.72$  kN. The corresponding EDF pulse values are  $F_{z2}=2.35$  N·s and  $F_{z4}=6.04$  N·s.

In LPEC-C<sub>p</sub>-E2, CA is connected in parallel with IW, and the front 2 and rear 3 EA act on the movable latch 7 (Fig. 2,c). Oppositely directed EDF act on each EA, the amplitudes of which are  $f_{z2,3m}=6.42$  kN. EDF act on CA, the amplitude of which is  $f_{z4m}=4.09$  kN. The corresponding values of EDF pulses acting on EA and CA are  $F_{z2,3}=1.98$  N·s and  $F_{z4}=4.07$  N·s.

In the LPEC-E-F with a fixed latch 7 and an internal power device 9, unidirectional action of all forces on the object of influence 8 is ensured. Amplitudes of the current density in IW  $j_{1m}=156$  A/mm<sup>2</sup>, in EA  $j_{2m}=385$  A/mm<sup>2</sup> (Fig. 2,d) However, the current in EA changes polarity to the opposite after 2 ms. The magnitude of the EDF pulse is  $F_{z2}=5.42$  N·s, and the EMF pulse is  $F_{z5}=3.49$  N·s.

In LPEC-C<sub>p</sub>-F, forces are transmitted to the object of influence 8 (Fig. 2,e) through the internal device 9 and the fixed retainer 7. The currents of density  $j_1$  in IW and  $j_4$  in CA have the form of a polar pulse with a short front and a long back front. Amplitudes of current densities IW  $j_{1m}=177.7$  A/mm<sup>2</sup>, CA  $j_{4m}=204.7$  A/mm<sup>2</sup>. The smaller value of the current amplitude in IW can be explained by the influence of the magnetic field on it from the side of the adjacent FA 5. CA is acted upon by repulsive EDF  $f_{z4}$ , the amplitude of which is  $f_{z4m}=13.03$  kN. The electromagnetic attraction  $f_{z5}$  acting on FA is much smaller and their amplitude is only  $f_{z5m}=1.19$  kN. The value of the EDF pulse is  $F_{z4}=12.25$  N·s, and the value of the EMF pulse is  $F_{z5}=1.2$  N·s. In this converter, the value of  $F_z$  is 1.21 times greater than in a LPEC with one CA and almost 2 times more than in a LPEC with one FA.

In LIEP-C<sub>p</sub>-E-F IW 1 interacts with FA 5 and with CA 4, which, in turn, interacts with EA 2 (Fig. 2,f). The currents in IW and CA have the form of an aperiodic polar pulse with a short leading edge and a long trailing edge. At the same time, the amplitudes of the current densities in IW and CA are different:  $j_{1m}=168.8$  A/mm<sup>2</sup>,  $j_{4m}=279.8$  A/mm<sup>2</sup>. The current amplitude in EA is  $j_{2m}=368.7$  A/mm<sup>2</sup>. The current in EA after reaching the maximum value decreases and changes polarity after 1 ms. Electromagnetic  $f_{z5}$  and electrodynamic  $f_{z4}$  forces during the entire work process maintain their polarities, and EDF  $f_{z2}$  acting on EA practically disappear after 1 ms. Repulsive EDF with amplitude  $f_{z4m}=5.58$  kN act on CA from side IW. FA is acted upon by EMF attraction  $f_{z5}$ , with amplitude  $f_{z5m}=0.92$  kN. The amplitude of the EDF acting on EA is  $f_{z2m}=7.48$  kN. The magnitude of the EDF impulse acting on CA is  $F_{z4}=6.59$  N·s, the magnitude of the EMF impulse acting on FA is  $F_{z5}=0.89$  N·s, the magnitude of the EDF impulse acting on EA is  $F_{z2}=2.45$  N·s.

Figure 3 presents the distributions of current densities  $j$  and magnetic field induction  $B$  in active elements at the moment of the maximum value of the current in IW for multi-armature LPEC of power purpose.

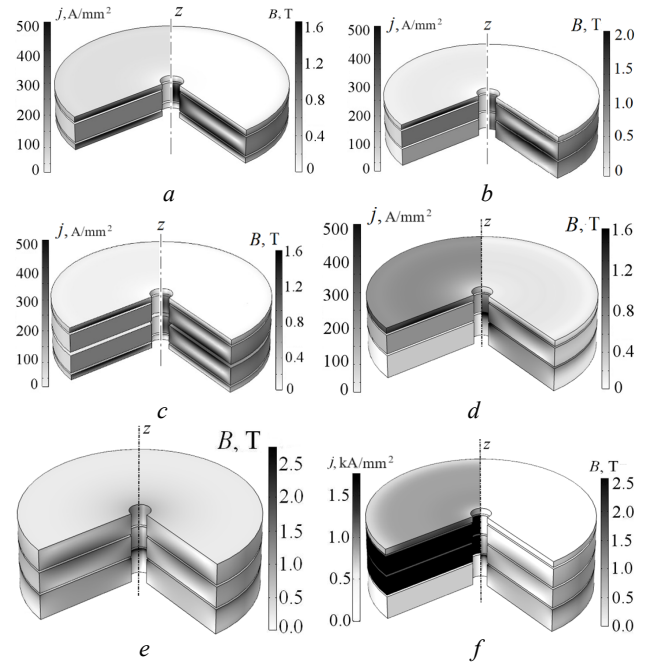


Fig. 3. Distributions of current densities  $j$  and magnetic field induction  $B$  in active elements at the moment of the maximum value of the current in IW for multi-armature LPEC of power purpose: LPEC-E2 (a), LPEC-C-E (b), LPEC-C-E2 (c), LPEC-E-F (d), LPEC-C-F (e), LPEC-C-E-F (f)

Figure 4 presents the electromechanical characteristics of LPEC-C<sub>p</sub>-E2 and LPEC-C<sub>p</sub>-F, which show that in the presence of FA, the amplitudes of the currents in IW decrease, which leads to a decrease in the EDF amplitude. But due to the slower attenuation of the currents, the magnitude of the force impulse not only does not decrease, but even increases.

In order to evaluate the most effective LPEC of the considered configurations, we will conduct a comparative analysis of them. As a basic option, we use the LPEC-E converter. At the same time, the amplitude of the excitation current density  $j_{1m}$  should be minimal, which is important for a pulse source, the amplitude  $f_{zm}$  and the magnitude of the force pulse  $F_z$  should be maximal, which is important for LPEC of power purpose, and the maximum induction of the scattering magnetic field on the defined circuit  $B_{ex m}$  should be minimal, which is important for service personnel on nearby electronic equipment.

Let's introduce the efficiency criterion  $K^*$ , which takes into account the specified electrical, power, and magnetic indicators in a relative form [20]:

$$K^* = \beta \left( \frac{\alpha_1}{j_{1m}} + \alpha_2 f_{zm}^* + \alpha_3 F_z^* + \frac{\alpha_4}{B_{ex m}^*} \right); \quad \sum_{n=1}^4 \alpha_n = 1, \quad (17)$$

where  $\beta$  – LPEC reliability coefficient;  $\alpha_n$  –  $n^{\text{th}}$  weighting factor of the corresponding LPEC indicator.

We believe that the reliability coefficient for LPEC without CA is  $\beta=1$ , and in the presence of CA it decreases to  $\beta=0.9$  due to the presence of a moving contact between IW and CA and its implementation in the form of a multi-turn coil.

We will apply five variants of the LPEC efficiency assessment strategy: I ( $\alpha_{1,4}=0.25$ ), II ( $\alpha_1=0.4$ ,  $\alpha_{2,3,4}=0.2$ ), III ( $\alpha_2=0.4$ ,  $\alpha_{1,3,4}=0.2$ ), IV ( $\alpha_3=0.4$ ,  $\alpha_{1,2,4}=0.2$ ), V ( $\alpha_4=0.4$ ,  $\alpha_{1,2,3}=0.2$ ). In the first option, all indicators are evaluated

equally, and in other options, priority is given to one of the indicators, which is evaluated twice as high as the others. Table 1 presents the relative values of  $K^*$  performance criteria of multi-armature LPEC for power purposes with different variants of their evaluation strategy.

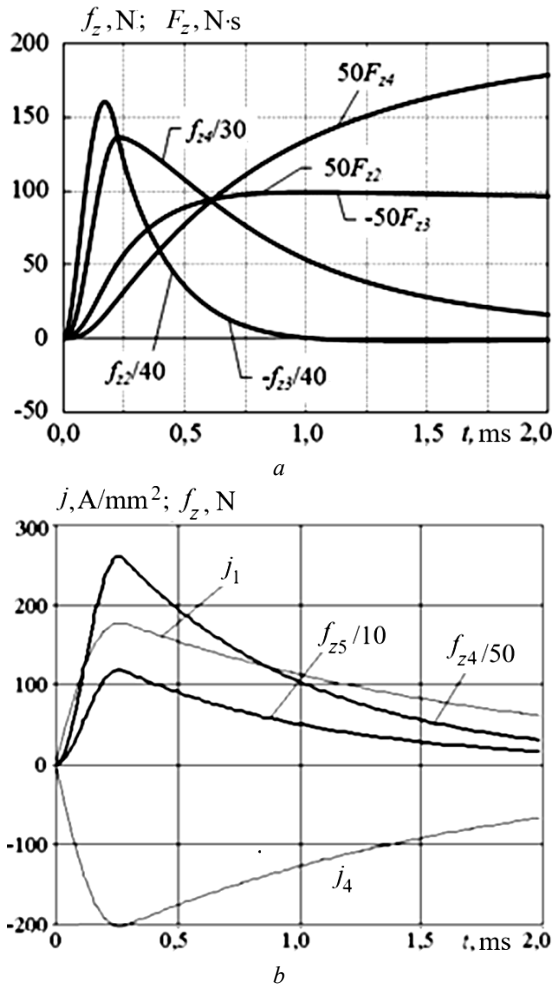


Fig. 4. Electromechanical characteristics LPEC-Cp-E2 (a), LPEC-Cp-F (b)

Table 1  
Relative values of  $K^*$  performance criteria of multi-armature LPEC for power purposes

LPEC	Option strategy				
	I	II	III	IV	V
LPEC-E2	1,569	1,393	1,659	1,544	1,679
LPEC-E-F	1,410	1,364	1,371	1,492	1,414
LPEC-C <sub>s</sub> -E	0,962	0,939	0,892	0,969	1,048
LPEC-C <sub>p</sub> -E	1,011	0,907	1,039	1,084	1,012
LPEC-C <sub>s</sub> -E2	4,028	3,348	3,442	3,438	5,883
LPEC-C <sub>p</sub> -E2	2,155	1,832	2,024	1,988	2,778
LPEC-C <sub>s</sub> -F	1,544	1,398	1,468	1,558	1,751
LPEC-C <sub>p</sub> -F	1,192	1,147	1,098	1,228	1,293
LPEC-C <sub>s</sub> -E-F	1,340	1,227	1,324	1,513	1,296
LPEC-C <sub>p</sub> -E-F	1,237	1,192	1,131	1,274	1,352

As can be seen from the Table 1, almost all multi-armature LPEC have higher efficiency compared to the basic single-armature converter. LPEC-C-E2 with two EA and CA is the most effective, and the converter in which CA and IW are connected in series shows higher performance compared to the converter in which CA and IW are connected in parallel. This high efficiency is

largely due to the reduced level of the scattering magnetic field  $B_{ex m}$  and the reduced amplitude of the excitation current density  $j_{1m}$ . LPEC with CA and EA provides a 1.46-fold increase in the EDF amplitude and a 2.09-fold increase in the EDF pulse, which is important for power purposes.

Consider the LPEC of high-speed purpose, for which the amplitude of the speed  $V_{zm}$  should be maximal. For this converter, we introduce the efficiency criterion  $K^*$ :

$$K^* = \beta \left( \frac{\alpha_1}{j_{1m}^*} + \alpha_2 V_{zm}^* + \frac{\alpha_3}{B_{ex m}^*} \right); \quad \sum_{n=1}^3 \alpha_n = 1. \quad (18)$$

We will apply four variants of the LPEC efficiency evaluation strategy: I ( $\alpha_{1,3}=0, (3)$ ), II ( $\alpha_1=0.5, \alpha_{2,3}=0.25$ ), III ( $\alpha_2=0.5, \alpha_{1,3}=0.25$ ), IV ( $\alpha_3=0.5, \alpha_{1,2}=0.25$ ). In the first option, all indicators are evaluated equally, and in other options, priority is given to one of the indicators, which is evaluated twice as high as the others. Since IW is stationary, we will consider only those LPEC variants of high-speed assignment that ensure the unidirectionality of all forces on the anchor at a stationary FA.

Table 2 presents the values of  $K^*$  efficiency criteria of high-speed multi-armature LPEC with different variants of their evaluation strategy in a relative form.

Table 2  
Relative values of  $K^*$  performance criteria of multi-armature LPEC for high-speed purposes

LPEC	Option strategy			
	I	II	III	IV
LPEC-E-F	0,972	0,996	0,846	1,082
LPEC-C <sub>p</sub> -F	1,096	1,020	1,074	1,198
LPEC-C <sub>s</sub> -F	1,311	1,294	1,144	1,494
LPEC-C <sub>p</sub> -E	0,855	0,781	0,899	0,886
LPEC-C <sub>s</sub> -E	0,912	0,941	0,845	0,952
LPEC-C <sub>p</sub> -E-F	0,763	0,776	0,837	0,680
LPEC-C <sub>s</sub> -E-F	1,075	1,419	0,999	1,119

The efficiency of multi-armature LPEC for high-speed performance in comparison with the basic version is significantly lower than for multi-armature LPEC for power purposes. This is primarily due to the fact that the speed of the moving combined armature does not increase significantly, and in some variants the LPEC even decreases due to the increased weight of such an armature.

Thus, it can be concluded that only for power LPEC, it is advisable to use multi-armature structures, and for high-speed LPEC, it is advisable to use traditional single-armature LPEC, which have a simpler design.

**Experimental studies of LPEC.** LPEC studies were conducted in laboratory conditions to verify the main theoretical propositions and calculation results. Experimental studies were performed for LPEC with parameters of active elements similar to the calculated ones. The experimental results were obtained with an aperiodic excitation pulse IW from CES with parameters  $U_0=250$  V,  $C_0=2500$   $\mu$ F.

The peculiarity of this technique was the simultaneous measurement of all indicators with the subsequent display of data on the screen of a digital oscilloscope and subsequent transfer of information to a personal computer for processing.

The CES voltage  $u_c(t)$  was measured using a PVP2150 digital meter, and the current  $i_1(t)$  in IW was measured using a 75ShSM shunt (Fig. 5).

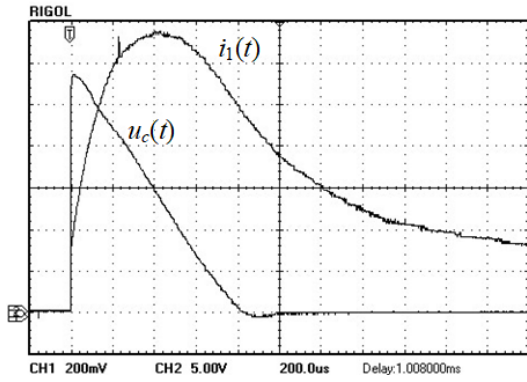


Fig. 5. Oscilloscope of voltage  $u_c(t)$  and current  $i_1(t)$  LPEC-C<sub>s</sub>-E

When studying the LPEC power purpose, the striker acts as an executive element, which carries out force impulses on the shock plate (Fig. 6,*a,b*). The T6000 piezo sensor was used to record the indicated pulses. The oscillogram of the force of the executive element  $f_z(t)$  on the shock plate and the current in IW  $i_1(t)$  is shown in Fig. 6,*c*.

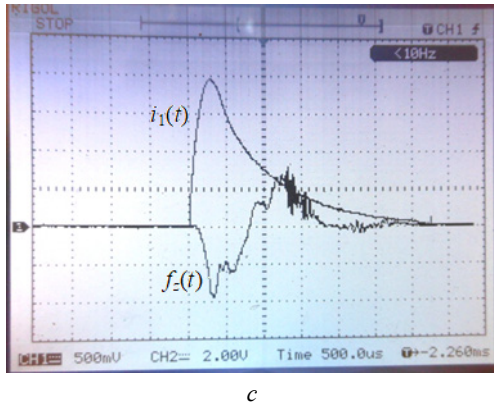
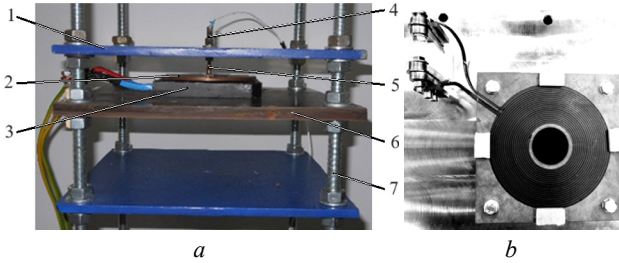


Fig. 6. Photo of the experimental setup (*a*), top view (*b*), oscillogram (*c*) of force  $f_z(t)$  and current  $i_1(t)$  LPEC-C<sub>p</sub>-E: 1 – impact plate; 2 – EA; 3 – IW; 4 – piezo sensor; 5 – fight; 6 – support plate; 7 – adjusting supports

When studying the LPEC for high-speed purposes, the executive element (a guide rod with a disk) makes a vertical movement (Fig. 7,*a*). Registration of the movement process is carried out using a variable resistor SP3-23, which is powered by a direct current source. The oscillogram of the movement of the executive element  $\Delta z$  and the current in IW  $i_1$  is presented in Fig. 7,*b*.

Measurement of the axial induction component of the LPEC  $B_z$  scattering magnetic field was performed using an induction sensor.

Tables 3, 4 present the experimental and calculated parameters of the LPEC for power and speed purpose: the amplitude of the current IW  $I_{1m}$ , the maximum axial component of the induction of the magnetic scattering field  $B_{zm}$ , the force  $f_{zm}$ , the speed  $v_{zm}$ .

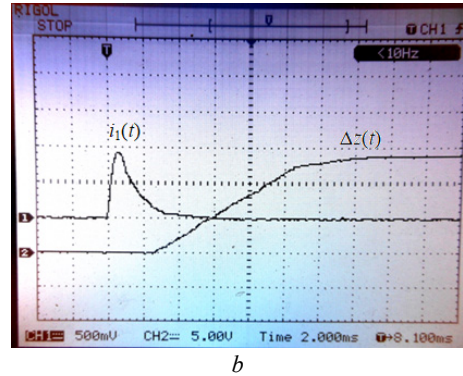
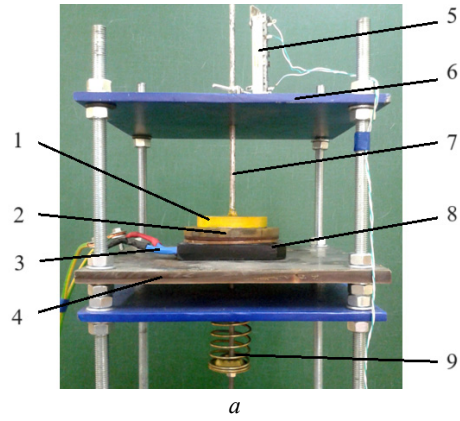


Fig. 7. Photo of the experimental setup (*a*), oscillogram (*b*) of displacement  $\Delta z(t)$  and current  $i_1(t)$  LPEC-C<sub>p</sub>-F: 1 – executive element; 2 – CA; 3 – current outlets IW; 4 – support plate; 5 – movement sensor; 6 – guide plate; 7 – guide pin of the executive element; 8 – IW; 9 – loading spring

Table 3  
Experimental (Exp.) and calculated (Calc.) parameters of LPEC for power purpose

LPEC	$I_{1m}$ , kA		$f_{zm}$ , kN		$B_{zm}$ , mT	
	Exp.	Calc.	Exp.	Calc.	Exp.	Calc.
LPEC-E	1.12	1.178	2.20	2.360	20	24
LPEC-F	0.57	0.610	0.38	0.408	17	20
LPEC-C <sub>p</sub>	1.37	1.430	3.55	3.815	28	32
LPEC-C <sub>s</sub>	0.96	1.001	1.74	1.830	30	34
LPEC-E-F	1.01	1.035	2.60	2.780	14	16
LPEC-C <sub>p</sub> -F	1.42	1.485	3.86	4.140	21	25
LPEC-C <sub>s</sub> -F	1.11	1.157	1.93	2.065	18	22
LPEC-C <sub>p</sub> -E	2.00	2.085	8.50	9.125	19	21
LPEC-C <sub>s</sub> -E	1.10	1.160	4.20	4.510	16	18
LPEC-C <sub>p</sub> -E-F	1.38	1.453	5.28	5.660	22	24
LPEC-C <sub>s</sub> -E-F	0.96	0.997	3.18	3.454	13	15

Table 4  
Experimental (Exp.) and calculated (Calc.) parameters of LPEC for high-speed purpose

LPEC	$I_{1m}$ , kA		$v_{zm}$ , m/s		$B_{zm}$ , mT	
	Exp.	Calc.	Exp.	Calc.	Exp.	Calc.
LPEC-E	1.01	1.050	3.0	3.5	22	25
LPEC-F	0.42	0.439	1.5	1.9	17	20
LPEC-C <sub>p</sub>	1.16	1.210	3.1	3.5	30	35
LPEC-C <sub>s</sub>	0.80	0.835	1.5	1.9	32	39
LPEC-E-F	0.86	0.899	1.6	1.8	14	16
LPEC-C <sub>p</sub> -F	1.15	1.200	3.5	3.9	13	15
LPEC-C <sub>s</sub> -F	0.73	0.760	2.1	2.5	9	11
LPEC-C <sub>p</sub> -E	1.62	1.695	3.7	4.0	20	23
LPEC-C <sub>s</sub> -E	0.89	0.925	2.0	2.5	19	21
LPEC-C <sub>p</sub> -E-F	1.12	1.165	3.5	4.1	48	53
LPEC-C <sub>s</sub> -E-F	0.76	0.785	2.5	3.0	15	18

Figure 8 presents the calculated and experimental currents  $i_1$  in IW LPEC-C<sub>p</sub>-E for power and speed purposes, which show that at the leading edge of the pulses, there is an almost complete coincidence of the calculated and experimental values, and at the trailing edge the difference between them increases.

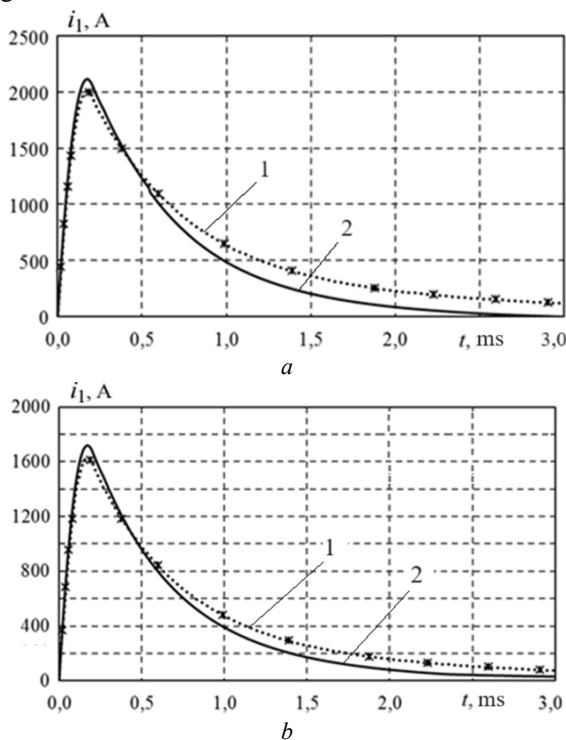


Fig. 8. Calculated (1) and experimental (2) currents  $i_1$  LPEC-C<sub>p</sub>-E power (a) and speed (b) purpose

In LPEC for power purposes, the relative errors between the calculated and experimental amplitudes of the current IW  $I_{1m}$  are 2.7-7 %, between the amplitudes of the force  $f_{zm}$  – 6.9-8.6 %, between the amplitudes of the axial component of the scattering magnetic field  $B_{zm}$  – 9.1-22.1 %.

In the high-speed LPEC, the relative errors between the calculated and experimental amplitudes of the current IW  $I_{1m}$  are 3.2-4.4 %, between the maximum speeds of the executive element  $v_{zm}$  – 6.7-19.5 %, between the amplitudes of the axial component of the scattering magnetic field  $B_{zm}$  – 10.4-22.2 %.

The obtained errors are acceptable for engineering studies in laboratory conditions and generally show the validity of the calculated results.

Based on the research conducted, a number of experimental models of electromechanical devices were developed and tested in laboratory conditions.

On the basis of LPEC-C-E2, a model of an electromagnetic UAV catapult was developed, which is characterized by reduced weight and size parameters and provides an increased departure speed. On the experimental model, it was established that when IW and CA are connected in parallel, the amplitudes of the excitation currents  $I_{1m}$  are 43 % higher, and the maximum speed is 60 % higher than when they are connected in series.

On the basis of LPEC-E-F, a model of a magnetic pulse press for ceramic powder materials was developed. The experimental model of the press provided a force pulse on the ceramic powder with amplitude of 85 MPa at

each work cycle. It was determined that impulse pressing of ceramic powders allows obtaining compacts, the density of which is 12 % higher than the density of samples obtained by static pressing.

On the basis of LPEC-E-F, a model of an electromechanical device for removing ice and snow deposits from a power line wire has been developed. The device generates horizontally directed forces of variable sign, which contributes to the effective removal of ice and snow deposits from the wire.

On the basis of LPEC-E2, a model of the device was developed for the destruction of information on a solid-state digital SSD drive in case of unauthorized access or on demand.

### Conclusions.

1. On the basis of a mathematical model implemented in the COMSOL Multiphysics software environment and taking into account interconnected electromagnetic, mechanical, and thermal processes, the features of electromechanical processes in multi-armature LPEC were established and their indicators were determined.

2. Practically all multi-armature LPEC for power purposes have higher efficiency compared to a single-armature converter. Thus, compared to LPEC with one electroconductive armature, LPEC with coiled and solid electroconductive armatures provides an increase in the amplitude of electrodynamic forces by 1.46 times and the magnitude of the impulse of electrodynamic forces by 2.09 times.

3. For high-speed LPEC, it is advisable to use traditional LPEC with one armature.

4. Experimental studies of LPEC with simultaneous measurement of electrical, mechanical and magnetic parameters were carried out. It was established that in laboratory LPEC for power and speed purposes, the calculated and experimental indicators of the current amplitudes of the inductor winding coincide with an accuracy of up to 7 %, for the amplitude of the force – up to 9 %, for the maximum speed of the executive element – up to 20 %, for the maximum value of the axial component of the magnetic field dispersion up to 22 %.

5. On the basis of multi-armature LPEC, models of an electromagnetic UAV catapult, a magnetic pulse press for ceramic powder materials, an electromechanical device for dumping ice and snow deposits from a power line wire, a device for destroying information on a solid-state digital SSD drive have been developed and tested.

**Conflict of interest.** The authors declare no conflict of interest.

### REFERENCES

1. Chemeris V.T. Impulse electromechanical converters of translational and rotational motion. *Energetics and energy saving*, 2012, no. 5(1), pp. 9-10. (Ukr).
2. Bissal A. *On the design of ultra-fast electro-mechanical actuators. Licentiate Thesis*. Stockholm, Sweden, 2013. 76 p. Available at: <https://www.diva-portal.org/smash/get/diva2:617236/FULLTEXT01.pdf> (accessed 15 May 2021).
3. Kondratiuk M., Ambroziak L. Concept of the magnetic launcher for medium class unmanned aerial vehicles designed on the basis of numerical calculations, *Journal of Theoretical and Applied Mechanics*, 2016, vol. 54, no. 1, pp. 163-177. doi: <https://doi.org/10.15632/jtam-pl.54.1.163>.

4. Go B., Le D., Song M., Park M., Yu I. Design and Electromagnetic Analysis of an Induction-Type Coilgun System With a Pulse Power Module. *IEEE Transactions on Plasma Science*, 2019, vol. 47, no. 1, pp. 971-976. doi: <https://doi.org/10.1109/TPS.2018.2874955>.
5. Reck B. First design study of an electrical catapult for unmanned air vehicles in the several hundred kilogram range. *IEEE Transactions on Magnetics*, 2003, vol. 39, no. 1, pp. 310-313. doi: <https://doi.org/10.1109/tmag.2002.805921>.
6. Torlin V.N., Vetrogon A.A., Ogryzkov S.V. Behavior of electronic units and devices under the influence of shock loads in an accident, *Automobile transport*, 2009, vol. 25, pp. 178-180. (Rus). Available at: <https://dSPACE.khadi.kharkov.ua/dSPACE/bitstream/123456789/8071/1/39.pdf> (accessed 15 May 2021).
7. Jeong Y., Lee H., Kim Y., Lee S. High-speed AC circuit breaker and high-speed OCR. *22nd International Conference and Exhibition on Electricity Distribution (CIRED 2013)*, Stockholm, 2013, pp. 1-4. doi: <https://doi.org/10.1049/cp.2013.0834>.
8. Kondratenko I.P., Zhylytsov A.V., Pashchyn N.A., Vasyuk V.V. Selecting induction type electromechanical converter for electrodynamic processing of welds. *Tekhnichna Elektrodynamika*, 2017, no. 5, pp. 83-88. (Ukr). doi: <https://doi.org/10.15407/techned2017.05.083>.
9. Soda R., Tanaka K., Takagi K., Ozaki K. Simulation-aided development of magnetic-aligned compaction process with pulsed magnetic field. *Powder Technology*, 2018, vol. 329, pp. 364-370. doi: <https://doi.org/10.1016/j.powtec.2018.01.035>.
10. Gorodzhia K.A., Podoltsev A.D., Troshchynckyi B.O. Electromagnetic processes in pulsed electrodynamic emitter to excite elastic vibrations in concrete structures. *Technical Electrodynamics*, 2019, no. 3, pp. 23-28. (Ukr). doi: <https://doi.org/10.15407/techned2019.03.023>.
11. Angquist L., Baudoin A., Norrga S., Nee S., Modeer T. Low-cost ultra-fast DC circuit-breaker: Power electronics integrated with mechanical switchgear. *2018 IEEE International Conference on Industrial Technology (ICIT)*, 2018, pp. 1708-1713. doi: <https://doi.org/10.1109/icit.2018.8352439>.
12. Puumala V., Kettunen L. Electromagnetic design of ultrafast electromechanical switches. *IEEE Transactions on Power Delivery*, 2015, vol. 30, no. 3, pp. 1104-1109. doi: <https://doi.org/10.1109/tpwrd.2014.2362996>.
13. Zhou Y., Huang Y., Wen W., Lu J., Cheng T., Gao S. Research on a novel drive unit of fast mechanical switch with modular double capacitors. *The Journal of Engineering*, 2019, vol. 2019, no. 17, pp. 4345-4348. doi: <https://doi.org/10.1049/joe.2018.8148>.
14. Bolyukh V.F., Shchukin I.S. Influence of limiting the duration of the armature winding current on the operating indicators of a linear pulse electromechanical induction type converter. *Electrical Engineering & Electromechanics*, 2021, no. 6, pp. 3-10. doi: <https://doi.org/10.20998/2074-272X.2021.6.01>.
15. Zhang M., Wang Y., Li P., Wen H. Comparative studies on two electromagnetic repulsion mechanisms for high-speed vacuum switch. *IET Electric Power Applications*, 2018, vol. 12, no. 2, pp. 247-253. doi: <https://doi.org/10.1049/iet-epa.2017.0396>.
16. Bolyukh V.F., Kocherga A.I. Multi-armature Electromechanical Converters of Impact-Force Action. *2021 IEEE International Conference on Modern Electrical and Energy Systems (MEES)*, 2021, pp. 1-6. doi: <https://doi.org/10.1109/MEES52427.2021.9598788>.
17. Vilchis-Rodriguez D.S., Shuttleworth R., Barnes M. Double-sided Thomson coil based actuator: Finite element design and performance analysis. *8th IET International Conference on Power Electronics, Machines and Drives (PEMD 2016)*, Glasgow, UK, 2016, pp. 1-6. doi: <https://doi.org/10.1049/cp.2016.0201>.
18. Bach J., Bricquet C. *Electric switching device with ultra-fast actuating mechanism and hybrid switch comprising one such device*. Schneider Electric Industries SAS. Patent US no. 8686814, 2014.
19. Bolyukh V.F., Katkov I.I. Influence of the Form of Pulse of Excitation on the Speed and Power Parameters of the Linear Pulse Electromechanical Converter of the Induction Type. *Volume 2B: Advanced Manufacturing*, Nov. 2019, 8 p. doi: <https://doi.org/10.1115/imece2019-10388>.
20. Bolyukh V.F., Kocherga A.A., Shchukin I.S. Comparative analysis of constructive types of combined linear pulse electromechanical converters. *Tekhnichna Elektrodynamika*, 2018, no. 4, pp. 84-88. (Ukr). doi: <https://doi.org/10.15407/techned2018.04.084>.

Received 24.11.2023

Accepted 30.12.2023

Published 01.05.2024

V.F. Bolyukh<sup>1</sup>, Doctor of Technical Science, Professor,  
 O.I. Kocherga<sup>1</sup>, PhD, Assistant Professor,  
<sup>1</sup> National Technical University «Kharkiv Polytechnic Institute»,  
 2, Kyrpychova Str., Kharkiv, 61002, Ukraine,  
 e-mail: vfbolyukh@gmail.com (Corresponding Author);  
 kocherga.oleksandr07@gmail.com

How to cite this article:

Bolyukh V.F., Kocherga O.I. Efficiency of multi-armature linear pulse electromechanical power and speed converters. *Electrical Engineering & Electromechanics*, 2024, no. 3, pp. 3-10. doi: <https://doi.org/10.20998/2074-272X.2024.3.01>